Optical absorption in alloys of Si, Ge, C, and Sn

B. A. Orner,[a] D. Hits, and J. Kolodzey
Department of Electrical Engineering, University of Delaware, Newark, Delaware 19716

F. J. Guarin
IBM Microelectronics Division, Hudson Valley Research Park, 1580 Route 52, Hopewell Junction, New York 12533

A. R. Powell
Advanced Technology Materials, 7 Commerce Drive, Danbury, Connecticut 06810

S. S. Iyer
SiBond L. L. C., Hudson Valley Research Park, 1580 Route 52, Hopewell Junction, New York 12533

(Received 13 December 1995; accepted for publication 29 February 1996)

Group IV semiconductor alloy systems offer promise as variable band gap alloys compatible with Si technology. Binary, ternary, and quaternary group IV alloys were grown by molecular beam epitaxy on Si substrates. The fundamental absorption edge was measured by Fourier transform infrared spectroscopy to obtain the optical band gap of the alloys, and the position of the fundamental absorption edge was observed to depend on the experimentally measured alloy composition. Our results indicate a variety of Si-rich group IV alloys with various band gaps are experimentally producible. © *1996 American Institute of Physics.* [S0021-8979(96)05411-4]

INTRODUCTION

The epitaxial growth of random alloys of group IV semiconductors on Si substrates is being investigated by many groups. These materials may permit widespread production of heterostructure devices compatible with existing Si technology.[1,2] Vegard's law predicts that the small atomic size of C compensates for Ge and Sn, which are larger than Si. Thus, alloy systems involving C could potentially be lattice matched to Si at certain compositions.

The $Si_{1-x}Ge_x$ system is miscible for all x, and $Si_{i-x}Ge_x$ alloys are easily formed. The solid solubilities of C in Si and Ge are low (at the melting points, 3×10^{18} cm^{-3} for Si, 1×10^{8} cm^{-3} for Ge).[3] The solid solubility of Sn in Si and Ge is likewise low (5×10^{19} cm^{-3} in Si, 5×10^{20} cm^{-3} in Ge).[4] Thus, most group IV alloys may not be formed at high temperature, but can be produced by low temperature growth techniques such as molecular beam epitaxy (MBE),[5] solid phase epitaxy,[6] and chemical vapor deposition.[7] The resulting materials are metastable and are not limited by the solid solubility of the solutes. The actual upper bound to the amount of C and Sn that can be incorporated into a crystalline group IV alloy is still under investigation, as is the experimental validation of Vegard's law for these systems.

An equally important issue is the behavior of the electronic band structure of these systems under alloying. Theoretical investigations have been accomplished for most of the group IV alloys. Studies involving linear and logarithmic interpolation of the Brillouin zone critical points using 3C–SiC and the cubic phase of the elements as endpoints generally indicate monotonic variations of the band gap and materials which are indirect in k space,[8] though some alloys containing Sn may be direct.[9] $Si_{1-y}C_y$ (Refs. 10–12) and $Si_{1-x-y}Ge_xC_y$ (Ref. 12) in particular have been studied using more complex approaches with counterintuitive results: In spite of the large band gap of diamond, these investigations predict that localized strain will result in a band gap decrease (perhaps with some oscillations) as the carbon content is increased. In fact, some alloys containing over 10% carbon are predicted to be semimetallic.

Experimental measurements of the band gap are plentiful for $Si_{1-x}Ge_x$ (Refs. 13 and 14) but sparse for $Si_{1-x-y}Ge_xC_y$ (Refs. 7, 15 and 16), $Si_{1-y}C_y$ (Ref. 17), and $Ge_{1-y}C_y$ (Refs. 18 and 19) with data being available for only a few compositions and temperatures. Experimental band gap measurements of other group IV alloys have, to our knowledge, not been previously reported. In this article, we report on the band gap of several such alloys.

GROWTH

$Si_{1-x}Ge_x$, $Si_{1-x-y}Ge_xC_y$, $Si_{1-x-y-z}Ge_xSn_yC_z$, and $Si_{1-x-y}Sn_xC_y$ alloys were epitaxially grown by MBE on Si(100) substrates polished on both sides. Separate elemental solid sources were used for each alloy component. The Ge and Sn were thermally heated in crucibles. The Si and C sources were crucible-less, with an electron beam used to heat the Si, and a pyrolytic graphite filament used as the C source. Substrate temperatures were 475 °C for all samples, and growth rates were approximately 1 μm/h.

ANALYSIS

X-ray diffraction (XRD) measurements indicated the presence of strained monocrystalline alloy layers. The presence of strained layers was expected based on the lattice constant predicted by Vegard's law and the metastable strain critical thickness of similarly strained Si-rich $Si_{1-x}Ge_x$/Si films.[1] The alloy lattice constant in the growth direction ranged from 5.431 to 5.461 Å, indicating nearly Si lattice matched alloy layers.

[a]Electronic mail: orner@ee.udel.edu

 0021-8979/96/79(11)/8656/4/$10.00

The Si, Ge, and Sn contents were measured by Rutherford backscattering spectrometry (RBS), which also indicated the layers were uniform in composition. The C content was inferred from the filament current, calibrated by XRD of binary alloys. The composition of the $Si_{0.92}Ge_{0.08}$ sample was inferred from the lattice constant obtained by XRD. Thickness, which ranged from 0.150 to 0.400 μm, was inferred from growth conditions and was found consistent with RBS measurements.

The optical absorption at photon energies near the band gap was measured at room temperature using Fourier transform infrared spectroscopy (FTIR). Measurements were obtained using a Nicolet 740 optical bench operating in the transmission mode with a quartz beam splitter and PbSe detector.

The transmission data of the samples were ratioed to transmission curves of substrate references to remove substrate absorption and front surface reflection effects. The index of refraction of the layer was expected to be different from that of the substrate. This resulted in an additive offset in the absorption data. This offset was removed by establishing as a zero absorption reference the transmission at photon energies well below the band gap where the absorption curve is flat.

Because the layers were thin, small values of the absorption coefficient (α) were difficult to measure. The noise level of the instrument was reduced by averaging the signal from multiple scans. A ratio of two backgrounds collected with the experimental configuration indicated a noise level within 0.05% of the 100% transmission line. At sample thicknesses of 0.15 μm, this permits measurements of absorption coefficients above 30 cm^{-1}.

Plot of $(\alpha h\nu)^2$ versus photon energy $h\nu$ are often used to determine the optical band gap of a direct semiconductor, and plots of $\sqrt{\alpha}$ vs $h\nu$ are likewise used to find the optical band gap and participating phonon energies of an indirect semiconductor. The region of interest in these plots, however, ordinarily lies well below $\alpha=30$. Because we could not observe this region, we have adopted the curve fitting approach described below.

The data were fit to theoretical fundamental absorption curves for both a direct band gap semiconductor,

$$\alpha=\begin{cases}\dfrac{K(h\nu_{\rm pt}-E_G)^{1/2}}{h\nu_{\rm pt}}, & h\nu_{\rm pt}\geqslant E_G,\\ 0, & h\nu_{\rm pt}<E_G\end{cases} \tag{1}$$

and an indirect band gap semiconductor,

$$\alpha_a=(h\nu_{\rm pt}+h\nu_{\rm pn}-E_G)^2, \tag{2}$$

$$\alpha_e=\exp\left(\frac{h\nu_{\rm pn}}{kT}\right)(h\nu_{\rm pt}-h\nu_{\rm pn}-E_G)^2, \tag{3}$$

$$\alpha=\begin{cases}K(\alpha_e+\alpha_a), & h\nu_{\rm pt}-h\nu_{\rm pn}\geqslant E_G\\ K\alpha_e, & h\nu_{\rm pt}+h\nu_{\rm pn}\geqslant E_G>h\nu_{\rm pt}-h\nu_{\rm pn},\\ 0, & h\nu_{\rm pt}+h\nu_{\rm pn}<E_G\end{cases} \tag{4}$$

where $h\nu_{\rm pt}$ is the photon energy, $h\nu_{\rm pn}$ is the energy of the dominant momentum-conserving phonon, E_G is the optical band gap, k is Boltzmann's constant, T is temperature, and K is a prefactor that includes several material and physical constants.

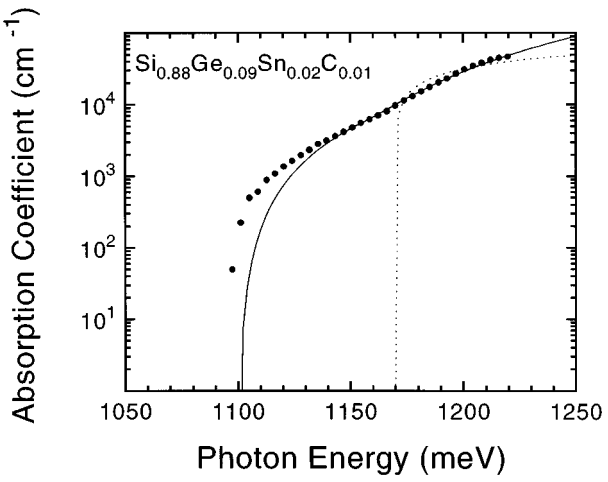

FIG. 1. Experimental fundamental absorption of a $Si_{0.88}Ge_{0.09}Sn_{0.02}C_{0.01}$ thin film (points), and best fit of data using an indirect band gap absorption edge (solid line) and direct band gap absorption edge (dotted line). These fits included absorption data from 1100 to 1230 meV.

These absorption functions were fit to the data using the Levenberg–Marquardt nonlinear curve fitting algorithm as implemented by the ORIGIN[20] software package. Both cases included E_G and K fitting parameters and the indirect case also included $h\nu_{\rm pn}$.

Figure 1 illustrates the result of direct and indirect band gap curve fits to the data of a $Si_{0.88}Ge_{0.09}Sn_{0.02}C_{0.01}$ sample over a broad energy range; the fit results to the other samples were similar in trends. The shape of the indirect curve matched the data better than the direct curve, though both departed at lower energies. To investigate the cause of this departure, the derivative of α with respect to photon energy was studied. This derivative should be linear for an indirect semiconductor; the sharp increase near 1160 meV shown in Fig. 2 suggests the onset of a second absorption mode, possibly a critical point energy.

In Fig. 3, an indirect curve could be fit well to the data below 1160 meV. (This fit differs from Fig. 1 in that the fit did not include data at energies above 1160 meV). The combination of an indirect curve at low energy and a second indirect curve at higher energies, though, best reflected the experimental data and minimized residual error (χ^2). We considered accounting for the second absorption curve by emission and absorption of an additional momentum conserving phonon in the alloy layer, as well as electron promotion to a second conduction band valley. However, each of the samples measured demonstrated a similar second indirect absorption curves, with onset energies which matched each other within 10 meV.

Therefore we attributed the higher energy indirect absorption curve to residual substrate absorption. This is consistent with the onset, near 1160 meV, of the TO phonon absorption assisted process in Si and the resultant increase in the slope of the absorption edge.[21] The sample spectra had been ratioed to substrates of the same lot number. Although

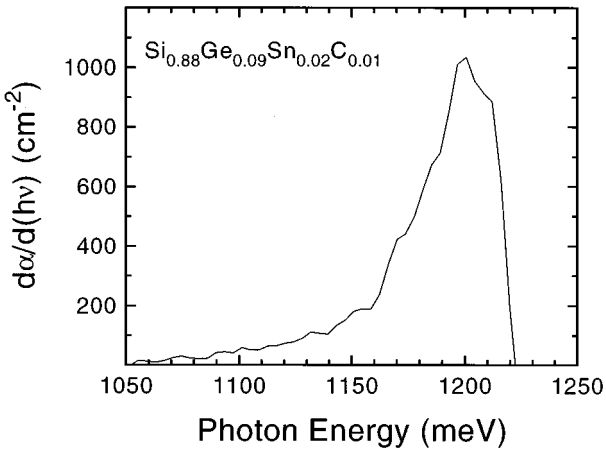

FIG. 2. The derivative of the experimental absorption data of the $Si_{0.88}Ge_{0.09}Sn_{0.02}C_{0.01}$ of Fig. 1. The sharp increase in the slope of the absorption curve near 1160 meV, which is characteristic of Si, was attributed to residual substrate absorption.

we were able to remove most of the substrate absorption, some substrate absorption is likely to remain due to slight thickness variations (Δd_{sub}) between substrates. Since the transmission varies with $\exp(-\alpha d)$, the effect of these thickness variations depended strongly on the substrate absorption coefficient (α_{sub}). Below 1160 meV, $\alpha_{\text{sub}}<0.2$ cm^{-1} and the impact of $\Delta d_{\text{sub}}\neq 0$ is negligible even for $\Delta d_{\text{sub}}=100$ μm. Above 1160 meV, α_{sub} rises rapidly (e.g., $\alpha_{\text{sub}}=100$ cm^{-1} at 1300 meV),[21] and significant residual substrate absorption occurs even if $\Delta d_{\text{sub}}=10$ μm. Although an additional indirect absorption curve at high energies (attributable to residual substrate absorption) improved the curve fit as shown by the solid line in Fig. 3, the substrate thickness could not be obtained with sufficient precision (under 1 μm)

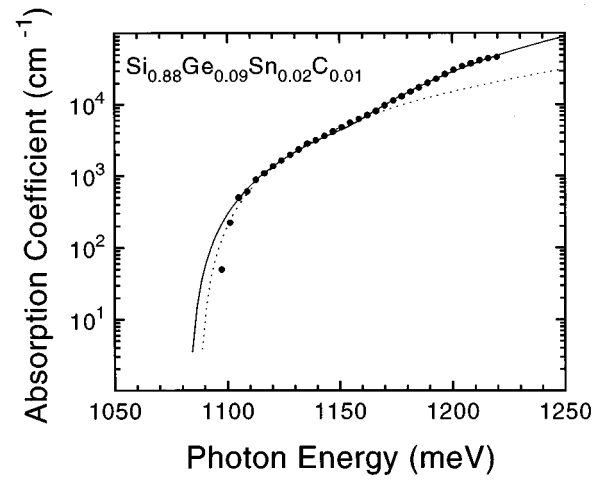

FIG. 3. The best fit of a theoretical indirect curve (dotted line) to the same experimental data as in Fig. 1 (points), with only data below 1160 meV included in the fit. An excellent fit was attained in this region, but the curve departed from the data above 1160 meV as indicated. The addition of another indirect curve representing the residual substrate absorption, beginning at 1160 meV resulted in an excellent fit across a wide range of absorption (solid line).

TABLE I. Optical band gaps of alloys. Fit results give the momentum conserving phonon energies determined by fitting a theoretical single-phonon fundamental indirect absorption model to experimental data from strained thin films; the stated band gap uncertainties are obtained from the fitting error and assume no uncertainty in the phonon energy. The strain corrected band gap was obtained by deducing the strain in the film from XRD measurements, and adding a correction factor to the fit results. This was compared to the linear estimate of the band gap obtained by interpolation of Brillouin zone critical points (see the text); uncertainties in this column arise from alloy composition uncertainties of ± 0.015 for Ge and ± 0.005 for C and Sn.

	Fit results		Strain corrected E_G (meV)	Linear estimate E_G (meV)
Composition	$h\nu_{\text{ph}}$ (meV)	E_G (meV)	E_G (meV)	E_G (meV)
$Si_{0.92}Ge_{0.08}$	43	1099±0.88	1113±0.88	1101±2
$Si_{0.91}Ge_{0.08}C_{0.01}$	54	1119±1.4	1127±1.4	1145±23
$Si_{0.88}Ge_{0.09}Sn_{0.02}C_{0.01}$	57	1145±1.1	1149±1.1	1147±21
$Si_{0.95}Sn_{0.04}C_{0.01}$	48	1145±7.7	1145±7.7	1159±23

to allow accurate modeling of the substrate absorption. To avoid introducing errors from this uncertainty, we restricted the curve fits to photon energies below 1160 meV. At those energies, we were confident that any effects of residual substrate absorption were negligible.

In general, the fitting algorithm converged upon multiple solutions. Local minima were found with $h\nu_{\text{ph}}\approx 5$ meV as well as those with $h\nu_{\text{ph}}\approx 50$ meV. Both of these resulted in similar values of χ^2. Previous studies of $Si_{1-x}Ge_x$ alloys[13] indicate that for $0.65<x<1.0$ the energy of the dominant phonon is nearly invariant at 48 meV. The phonon energy then drops over a narrow composition range and again remains nearly constant at 23 meV for $0<x<0.35$. This trend for $Si_{1-x}Ge_x$ optical phonons has been confirmed in photolumiscence studies.[22] The alloys in our investigation all contain over 65% Si, thus we expect phonon energies near 50 meV. Solutions requiring $h\nu_{\text{ph}}\approx 5$ were rejected for their inconsistency with this expectation. After rejecting such solutions, a unique solution remained for each sample.

The E_G and $h\nu_{\text{ph}}$ parameters of Eq. (4) exhibit a strong mutual dependence at the experimentally observable values of α. As a result, the fitting uncertainties of these two parameters were similar, though this uncertainty was still under 25 meV for all samples except the $Si_{0.95}Sn_{0.04}C_{0.01}$ sample. If the alloys studied here do in fact behave similar to $Si_{1-x}Ge_x$ alloys and the $h\nu_{\text{ph}}$ is considered known, the band gap uncertainties are reduced to the values of Table I.

Figure 4 illustrates the resulting curve of the best fit to the experimental data of each sample. In each case, the indirect model provided the best fit in terms of both form and residual error. The parameters from these curve fits are summarized by Table I. The results for the $Si_{0.92}Ge_{0.08}$ sample agreed well with established experimental values.[21]

Because the alloys were nearly lattice matched to the substrate, strain effects were minimized, but still present. Following St. Amour *et al.*,[16] we obtained the unstrained alloy band gap by computing a strain correction factor. We obtained the alloy lattice constant in the growth direction from XRD, estimated Poisson's ratio (ν) for each alloy by

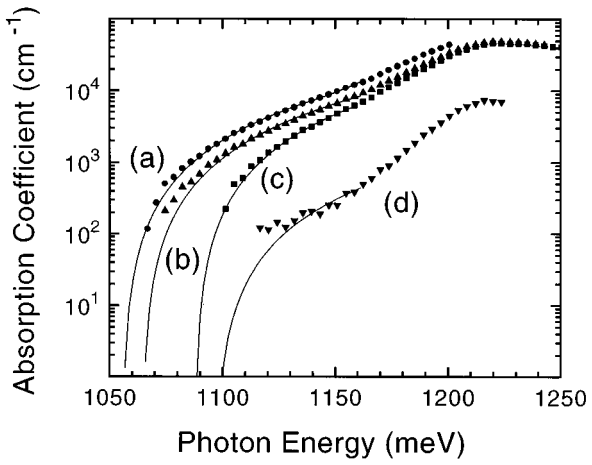

FIG. 4. Experimental fundamental absorption (points) and curve of best fit of thin films of (a) $Si_{0.92}Ge_{0.08}$, (b) $Si_{0.91}Ge_{0.08}C_{0.01}$, (c) $Si_{0.88}Ge_{0.09}Sn_{0.02}C_{0.01}$, and (d) $Si_{0.95}Sn_{0.04}C_{0.01}$. An indirect absorption curve resulted in the best fit in each case.

interpolating between the elemental values (ν=0.10 for diamond, $\nu\approx$0.28 for Ge, Si, and Sn),[21] and computed a biaxial strain in the plane of the heterointerface. Then, the deformation potential was assumed to be similar to that of the $Si_{1-x}Ge_x$ system ($\Delta E_G\approx-11.7$ eV/unit strain),[23] and the resulting correction factors were added to our experimental band gaps (Table I).

In an approach similar to Soref,[8,9] the experimental band gaps of each sample were compared to an estimate based on linear interpolations of Brillouin zone X, L, and Γ critical point conduction band energies,

$$E_G=\min_{i=X,L,\Gamma}\left[E^i_{\mathrm{Si}}(1-x-y-z)+E^i_{\mathrm{Ge}}x+E^i_{\mathrm{Sn}}y+E^i_{\mathrm{C}}z\right], \tag{5}$$

where the E^i are the conduction band energy minima at zone position i with respect to the valance band maximum at Γ, and x, y, and z are the atomic fractions of Ge, Sn, and C. Endpoints were based primarily on experimental observations, supplemented by psuedopotential calculations, of the band structure of the diamond phase of the pure elements.[21] This approach predicted conduction band minima at the X points for the composition of all the samples in this study, and band gap energies that were generally in good agreement with our experimental results. The critical point energy near the X point is larger for Sn than for Si, resulting in an increase in the band gap energy when Sn is added to a Si-rich alloy. This was experimentally observed.

CONCLUSION

In conclusion we have grown a variety of random crystalline alloys of Si, Ge, C, and Sn by MBE. The optical band gap was deduced by measuring the fundamental absorption edge of the alloys. These alloys were found to be indirect materials at the compositions studied, and the band gap was found to be nearly linearly dependent on composition. This investigation supports the use of these alloys as variable band gap materials compatible with existing Si technology.

ACKNOWLEDGMENTS

We are grateful to C. P. Swann, Department of Physics and Astronomy, University of Delaware, for his assistance in performing RBS measurements. This work is supported by AASERT Grant No. F49620-92-J-0340, AFOSR Grant No. AFOSR 91-0370, and ONR Grant No. N00014-93-1-0393.

[1] J. C. Bean, Proc. IEEE **80**, 571 (1992).
[2] R. A. Soref, Proc. IEEE **81**, 1687 (1993).
[3] R. I. Scace and G. A. Slack, J. Chem. Phys. **30**, 1551 (1959).
[4] A. G. Milnes, *Deep Impurities in Semiconductors* (Wiley, New York, 1973).
[5] K. Eberl, S. S. Iyer, S. Zollner, J. C. Tsang, and F. K. LeGoues, Appl. Phys. Lett. **60**, 3033 (1992).
[6] J. W. Strane, H. J. Stein, S. R. Lee, B. L. Doyle, S. T. Picraux, and J. W. Mayer, Appl. Phys. Lett. **63**, 2786 (1993).
[7] P. Boucaud, C. Francis, F. H. Julien, J. M. Lourtoiz, D. Bouchier, S. Bodnar, B. Lambert, and J. Regolini, Appl. Phys. Lett. **64**, 875 (1994).
[8] R. A. Soref, J. Appl. Phys. **70**, 2470 (1991).
[9] R. A. Soref and C. H. Perry, J. Appl. Phys. **69**, 539 (1991).
[10] A. A. Demkov and O. F. Sankey, Phys. Rev. B **48**, 2207 (1993).
[11] J. Gryko and O. F. Sankey, Phys. Rev. B **51**, 7295 (1995).
[12] J. Xie, K. Zhang, and X. Xie, J. Appl. Phys. **77**, 3868 (1995).
[13] R. Braunstein, A. R. Moore, and F. Herman, Phys. Rev. **109**, 695 (1958).
[14] E. R. Johnson and S. M. Christian, Phys. Rev. **95**, 560 (1954).
[15] J. Kolodzey, P. R. Berger, B. A. Orner, D. Hits, F. Chen, A. Khan, X. Shao, M. Waite, S. I. Shah, C. P. Swann, and K. M. Unruh, J. Cryst. Growth **157**, 386 (1995).
[16] A. St. Amour, C. W. Liu, J. C. Sturm, Y. Lacroix, and M. L. W. Thewalt, Appl. Phys. Lett. **67**, 3915 (1995).
[17] K. Brunner, K. Eberl, and W. Winter, Phys. Rev. Lett. **76**, 303 (1996).
[18] J. Kolodzey, P. A. O'Neil, S. Zhang, B. Orner, K. Roe, K. Unruh, C. Swann, M. Waite, and S. I. Shah, Appl. Phys. Lett. **67**, 1865 (1995).
[19] B. A. Orner, A. Khan, D. Hits, F. Chen, K. Roe, J. Pickett, X. Shao, R. G. Wilson, P. R. Berger, and J. Kolodzey, J. Electron. Mater. **25**, 297 (1996).
[20] ORIGIN, Microcal Software, Incorporated.
[21] *Landolt-Bornstein: Numerical Data and Functional Relationships in Science and Technology, Group III*, edited by O. Madelung (Springer, Berlin, 1982), Vol. 17a.
[22] J. Weber and M. I. Alonso, Phys. Rev. B **40**, 5683 (1989).
[23] C. G. Van De Walle and R. M. Martin, Phys. Rev. B **34**, 5621 (1986).